



Universidad Autónoma
de Madrid

Biblos-e Archivo
Repositorio Institucional UAM

Repositorio Institucional de la Universidad Autónoma de Madrid

<https://repositorio.uam.es>

Esta es la **versión de autor** del artículo publicado en:
This is an **author produced version** of a paper published in:

Journal of Chemical Technology and Biotechnology 95.7 (2020): 1926-1935

DOI: <https://doi.org/10.1002/jctb.6306>

Copyright: © 2019 Society of Chemical Industry

El acceso a la versión del editor puede requerir la suscripción del recurso
Access to the published version may require subscription

1
2
3 **1 Ionic liquids removal by sequential photocatalytic and biological oxidation**
4

5
6 **2 Short title: ILs removal by photocatalytic-biological oxidation**
7

8
9 **3 E. Gomez-Herrero^{*}, M. Tobajas, J.J. Rodriguez, A. F. Mohedano**
10

11 **4 Department of Chemical Engineering, Faculty of Science, Universidad Autónoma de**
12
13 **5 Madrid, Campus de Cantoblanco, 28049 Madrid, Spain.**
14

15
16 **6 Corresponding author: Tel.: +34 914973525**
17

18
19 **7 E-mail address: *esther.gomezh@uam.es***
20
21
22
23
24
25
26
27
28
29
30
31
32
33
34
35
36
37
38
39
40
41
42
43
44
45
46
47
48
49
50
51
52
53
54
55
56
57
58
59
60

Abstract

BACKGROUND: The industrial application of ionic liquids (ILs) can induce the generation of wastewater and their release into the aquatic media. ILs can be efficiently removed by advanced oxidation processes (AOPs), which are expensive to implement. An alternative, using solar photocatalysis and biological degradation in combination, was used here to remove 1-hexyl-3-methylimidazolium chloride (HmimCl) and 1-butyl-4-methylpyridinium chloride (BmpyrCl). The chemical pretreatment allowed the ILs to be converted into byproducts for easier biodegradation in a sequential batch reactor (SBR).

RESULTS: Photocatalytic degradation, using 0.25 g TiO₂ L⁻¹ and 600 W m⁻² solar radiation for 24 h, allowed a complete ILs removal and a partial mineralization of the organic matter, 28% for Bmpyr⁺ and 35% for Hmim⁺. A degradation pathway based on the byproducts identified was proposed for each IL. The reaction effluents were submitted to a biological treatment in a SBR, using organic loading rates of 0.18–0.2 kg COD kg⁻¹ VSS d⁻¹ and a biomass concentration of 3.5 g VSS L⁻¹ in 8 h cycles. The combined treatment allowed highly efficient removal of organic matter (TOC conversion exceeded 75% for HmimCl and 78% for BmpyrCl).

CONCLUSION: Solar photocatalytic oxidation efficiently removed ILs and produced more biodegradable and less ecotoxic effluents. Biological oxidation increased TOC and COD removal to more than 75% for the overall treatment. Combining solar photocatalysis and biological degradation therefore provided an effective system for IL removal.

Keywords

Ionic liquid, Solar photocatalytic oxidation, Biological degradation, Ecotoxicity, Sequencing batch reactor.

1. Introduction

Ionic liquids (ILs) are molten salts formed by an organic cation and an organic or inorganic anion that confer them unique properties such as low flammability, low vapor pressure, and high chemical and thermal stability.^{1,2} Some cation–anion pairs are of especial industrial interest^{3–5} and have been efficiently used in catalysis and separation processes.^{6–8} ILs have been deemed “green” compounds by virtue of their low vapor pressure preventing reaching the atmosphere as pollutants, a property that makes them effective alternative to conventional volatile organic solvents.^{9,10} However, the environmentally friendly image of ILs has been questioned on the grounds of their high to moderate environmental toxicity and low biodegradability, which can result in water pollution.^{11–13} A number of toxicity assays have been developed in recent decades for an expeditious, reproducible evaluation of the effects of pollutants on the aquatic environment. Toxicity tests with organisms from different trophic levels including bacteria, algae, plants or even mammalian cells have revealed that some ILs are even more toxic than conventional organic solvents.^{9,14–16} Because ILs can penetrate cell membranes and accumulate in the lipid bilayer, their toxicity usually increases with increasing hydrophobicity and decreasing polarity.¹⁴ Also, the high thermal and chemical stability of these compounds, and their slow biological degradation, makes it difficult to develop safe, sustainable ILs.^{15,16}

Developing cost-effective treatments for IL removal is essential to avoid their possible transfer from industrial wastewater to aquatic media. Advanced oxidation processes (AOPs) including Fenton-based reactions, electrolytic oxidation and ozonation, which are based on the *in situ* production of hydroxyl radicals (HO•) with a strong oxidizing power, have proved highly effective for IL removal.^{17–19} Photocatalysis appears to be the most environmentally friendly choice as it uses an external component (UV or solar radiation)

to produce the radicals.²⁰ Photocatalytic oxidation uses a catalyst, which acts as a semiconductor and can be excited producing “electron–hole” pairs.²¹ The charges thus generated promote a redox reaction on the photocatalyst surface and facilitates adsorption of the pollutant as a result. Photocatalysis has proved an effective treatment for removing pollutants from aqueous media.^{22–24} **Table 1** summarizes the main contributions to IL degradation by photocatalytic oxidation. In general, complete IL removal was achieved as well as acceptable removal of total organic carbon (TOC). Photocatalytic activity increases with increasing length of the cation alkyl chain in imidazolium-based ILs; by contrast, ILs with a small molecular mass are highly stable.

Table 1. Summary of ILs removal by photocatalytic oxidation.

Ionic Liquids	Operating conditions	Main results	Reference
BmimCl, BmimBF ₄ HmimCl, HmimBF ₄ OmimCl, OmimBF ₄ DmimCl, DmimBF ₄ EeimBF ₄ Mim (Control)	TiO ₂ : 500 mg L ⁻¹ IL: 1 mM UV light (1000 W Xe lamp) 6h	IL conversion Bmim: 99.9% (360 min) Mim: 99.9% (180 min) Omim, Hmim: 23% Eeim: 15%	25
Imidazolium, pyridinium, phosphonium and ammonium ILs	TiO ₂ : 200 mg L ⁻¹ IL: 100 mg L ⁻¹ UV light (153 W m ⁻² 20W) 5h	Degradation rate depends on the cation and anion of the IL. Higher stability for ILs with lower mass	26
EmimBr EmimPF ₆ BmimBF ₄	TiO ₂ or Pt/TiO ₂ : 0.1 g IL: 20 mg L ⁻¹ UV light (300 W Xe lamp) – 24h	Cation removal: EmimPF ₆ and EmimBF ₄ : 99.9% (Pt/TiO ₂ and TiO ₂) EmimBr: 87.8 % (Pt/TiO ₂) Anion removal: Br ⁻ and BF ₄ ⁻ : 99.9% PF ₆ ⁻ < 20%	27

MimHSO ₄ EmimHSO ₄	TiO ₂ : 200 mg L ⁻¹ IL: 10 mg L ⁻¹ UV light (40 W lamp) 5 min - 4h	Cation removal : 99.9% TOC: 99.9% (240 min)	28
EpyrBF ₄ BpyrBF ₄ HpyrBF ₄ BmpyrBF ₄ BpyrBr BmpyrBr BpyrCl CppyrCl	TiO ₂ : 200 mg L ⁻¹ IL: 20 mg L ⁻¹ UV light (40 W lamp) 6h	IL removal: 99.9% (30 min) TOC: 100% (120-150 min) Anion part affects the transformation pathway	29
BmimCl BmimPF ₆ BmimNTf ₂ BmmimCl BmmimNTf ₂	SiTi: 0.7 g L ⁻¹ IL: 20 mg L ⁻¹ VIS light (125 W Hg vapor lamp) and UV lamp 2h	IL removal: BmimCl (UV): 50% BmimCl (VIS): 45% Minor role of the anion on degradation: Cl ⁻ > PF ₆ ⁻ > NTf ₂ ⁻ . – CH ₃ substituent decreases photocatalytic activity	30
EmimCl BmimCl DmimCl BmimBF ₄ BmimFAP AllylmimCl EtOHmimCl BmpyrCl	TiO ₂ : 75 mg L ⁻¹ IL: 20 mg L ⁻¹ Sunset simulator (Xe Lamp 450 W m ⁻²) 10h	ILs removal: 99.9% TOC > 90% (Unless FAP anion: 20%) Cation degradation rate: (Dmim > Bmim > Emim) Minor role of the anion on degradation	31

Preserving the green image of ILs requires using highly efficient biological treatments for their removal.³² Unfortunately, their low biodegradability and moderate ecotoxicity complicates their microbial degradation.^{33,34} Intensification techniques such as cometabolism or bioaugmentation have been used in combination with biological treatments based on activated sludge to increase the efficiency with which these microbially recalcitrant compounds can be removed.^{35,36} The joint use of intensification

1 techniques and appropriate acclimation strategies have in fact enabled the treatment of
2
3
4
5
6
7
8
9
10
11
12
13
14
15
16
17
18
19
20
21
22
23
24
25
26
27
28
29
30
31
32
33
34
35
36
37
38
39
40
41
42
43
44
45
46
47
48
49
50
51
52
53
54
55
56
57
58
59
60

1 techniques and appropriate acclimation strategies have in fact enabled the treatment of
2 recalcitrant pollutants in biological reactors.

3 Combining a chemical oxidation pretreatment with biological degradation allows
4 pollutants, recalcitrant to microbial oxidation, to be completely removed,^{37,38} and organic
5 matter to be efficiently mineralized while ensuring that an adequate amount of carbon
6 remains in order to maintain the organic loading rate of a biological reactor.³⁹ The
7 combination of a Fenton reaction and biological degradation in an SBR allowed
8 successful removal of pesticides and pharmaceuticals,^{40–42} and also of ionic liquids in
9 aqueous media⁴³ with overall chemical oxygen demand (COD) removal and TOC
10 conversion above 80% (i.e., higher than the degradation produced in each treatment
11 individually). Nevertheless, to the best of our knowledge, photocatalytic degradation and
12 advanced biological treatments in SBRs have scarcely been used for IL removal. Solar
13 photocatalysis may be an effective choice for the chemical degradation of ILs and partial
14 mineralization of organic matter thanks to the low environmental impact of solar light as
15 inducer of “electron–hole” pairs.^{31,44}

16 The aim of this work was to assess the efficiency of a sequential process involving
17 photocatalytic degradation and biological treatment for the removal of 1-hexyl-
18 imidazolium-chloride (HmimCl) and 1-butyl-4-methylpyridinium chloride (BmpyrCl)
19 from aqueous solution. An optimal catalyst and ILs concentration were used in the
20 chemical oxidation step to obtain biodegradable and scarcely ecotoxic effluents for
21 subsequent biodegradation in a SBR with increased organic matter conversion in terms
22 of COD removal and TOC mineralization. A reaction pathway for the photocatalytic
23 degradation of HmimCl and BmpyrCl based on the structure of their main byproducts is
24 proposed.

2. Materials and Methods

2.1. Chemicals

The ionic liquids (1-hexyl-3-methylimidazolium chloride and 1-butyl-4-methylpyridinium chloride) and all other chemicals were purchased from Sigma–Aldrich. The properties of the photocatalyst (Aeroxide[®] TiO₂-P25 from Evonik-Degussa) are described in detail elsewhere.³¹

2.2. Photocatalytic and biological oxidation

The photocatalytic degradation of HmimCl and BmpyrCl was performed in Pyrex glass batch slurry reactors (500 mL) under simulated solar radiation. Aqueous solutions with an IL concentration of 0.35 g L⁻¹ were mixed with 0.1–1.0 g TiO₂ L⁻¹ to examine the influence of the catalyst concentration. The reactors were equipped with aerators and magnetic stirrers to disperse the catalyst. The dispersions formed were allowed to stand under stirring in the dark overnight in order to ensure they reached adsorption equilibrium. Then, photocatalytic tests were conducted at 35 °C for 24 h in a Suntest XLS+ solar simulator from ATLAS equipped with a xenon lamp (320–800 nm), using a fixed irradiation intensity of 600 W m⁻². Photolysis tests in the absence of photocatalyst were also conducted to assess the stability of the ILs under solar light. IL concentrations, TOC and COD were determined from samples withdrawn at different reaction times, after passing them through Albert FV-C filters of 45 µm pore size. Photocatalytic oxidation tests were performed by duplicate. Data reported are average values of two experiments with their standard deviation.

1 The inoculum used for biodegradability testing and biological oxidation was collected
2 from a municipal wastewater treatment plant. The sludge was maintained at 25 °C in an
3 SBR and fed with sodium acetate and glucose as carbon sources. The medium was
4 supplied with ammonium sulfate, phosphoric acid and mineral salts as nitrogen,
5 phosphorous and micronutrient source, respectively, in a COD:N:P:micronutrient
6 proportion of 100:5:1:0.05 (w/w).

7 The biodegradability of the effluents from the photocatalytic oxidation of the ILs was
8 assessed with the fast biodegradability test on an LSS respirometer.⁴⁵ Effluent samples
9 were held in 1 L vessels, placed in a thermostatic bath (25 °C), stirred, aerated and mixed
10 with activated sludge (350 mg L⁻¹) for 24 h. The resulting specific oxygen uptake rate
11 (SOUR, mg O₂ g⁻¹ VSS h⁻¹) was determined by using an oximeter to measure the decrease
12 in dissolved oxygen concentration between two set points. Samples were periodically
13 collected from the vessels for TOC measurements.

14 The biological treatment was conducted in a 3 L SBR at a controlled temperature (25 °C)
15 under stirring at 200 rpm. The SBR was equipped with an air diffuser, a dissolved oxygen
16 probe and peristaltic pumps to feed and unload the bioreactor. Each operating cycle, 8 h
17 in length, comprised a filling and anoxic stage (0.5 h), aeration (7 h), and settling and
18 drawing (0.5 h). The organic loading rate was maintained at 0.18–0.2 kg COD kg⁻¹ VSS
19 d⁻¹ and the biomass concentration at 3.5 g VSS L⁻¹. The effluents from the photocatalytic
20 oxidation of the ILs were used as the sole carbon sources. Each aqueous solution was
21 supplied with nitrogen, phosphorous and mineral salts for microbial growth. TOC, COD
22 and the concentrations of organic byproducts and inorganic nitrogen species were
23 determined in samples withdrawn at the end of the cycle, as well as during a whole

aeration step in the last biological oxidation cycle. A scheme of photocatalytic and biological reactors is depicted in Figure 1.

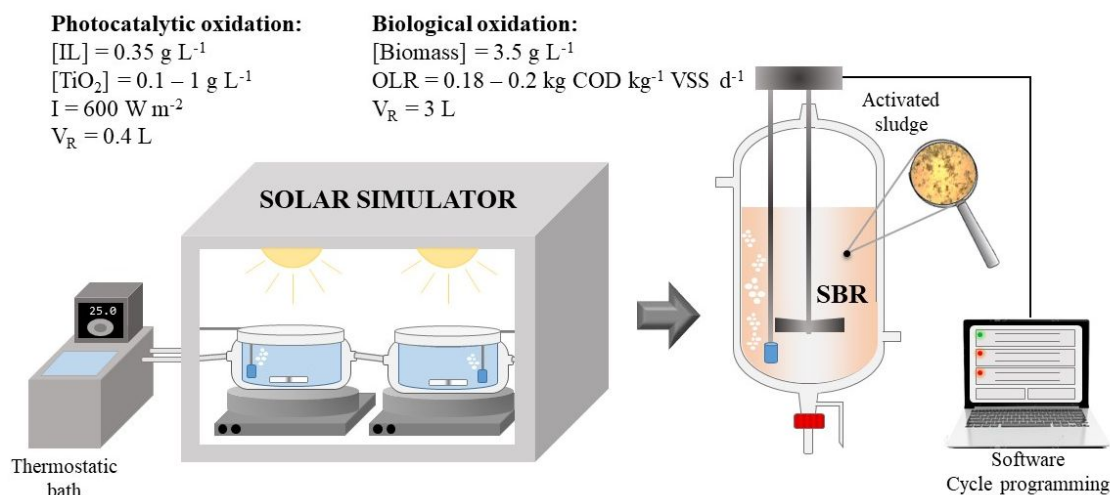


Figure 1. Scheme of photocatalytic and biological reactors setup.

2.3. Analytical methods

TOC was measured on a Shimadzu TOC-VCSH analyzer. Biomass concentration and COD were determined by following APHA procedure 2540E and 5220A, respectively. IL concentrations were quantified with a Varian Prostar 325 HPLC instrument equipped with a UV-Vis detector. A Synergy 4 mm Polar-RP 80 A column (15 cm length \times 4.6 mm diameter) from Phenomenex was used as stationary phase and phosphate buffer as mobile phase. The flow rate through the column was maintained at 0.75 mL min^{-1} and a wavelength of 280 nm was used for IL detection. Short-chain organic acids, nitrate and nitrite were determined by ion chromatography with chemical suppression on a Metrohm 790 IC, using a Metrosep A sup 2-250 column (25 cm length \times 4 mm i.d.) as stationary phase and an aqueous solution containing 1 mM NaHCO_3 and 3.2 mM Na_2CO_3 and circulated at a constant flow rate of 7 mL min^{-1} as mobile phase. Reaction byproducts

were detected by HPLC/MS on an Agilent Quadrupole LC/MS instrument using an ACE Excel 3 C-18-amide column (15 cm length \times 4.6 mm diameter) as stationary phase and an aqueous solution of formic acid (0.1 %) at a constant flow rate of 0.5 mL min⁻¹ as mobile phase. Mass spectrometry in the ESI + ionization mode was used at a drying gas flow rate of 9 L min⁻¹. The ecotoxicity of the initial IL solutions and the effluents from their photocatalytic degradation was assessed with the standard toxicity test based on the luminescence activity of the marine bacterium *Vibrio fischeri*. After 15 min of exposure to the pollutants, a Microtox[®] analyzer from SDI was used to measure the bioluminescence decrease, and toxicity was assessed in terms of EC₅₀ for the initial solutions and IC₅₀ for the effluents upon chemical oxidation.

3. Results and discussion

Figure 2 shows the variation of IL concentration during the photocatalytic oxidation of BmpyrCl and HmimCl in aqueous solutions irradiated with solar light. Prior to the photocatalytic experiments, the adsorption capacity of TiO₂ was checked in dark. Since photocatalytic oxidation occurred on the surface of the catalyst, an adsorption test was used to determine to what extent the ILs were removed by oxidation. The photostability of the ILs under solar irradiation was assessed by photolysis in absence of the photocatalyst.

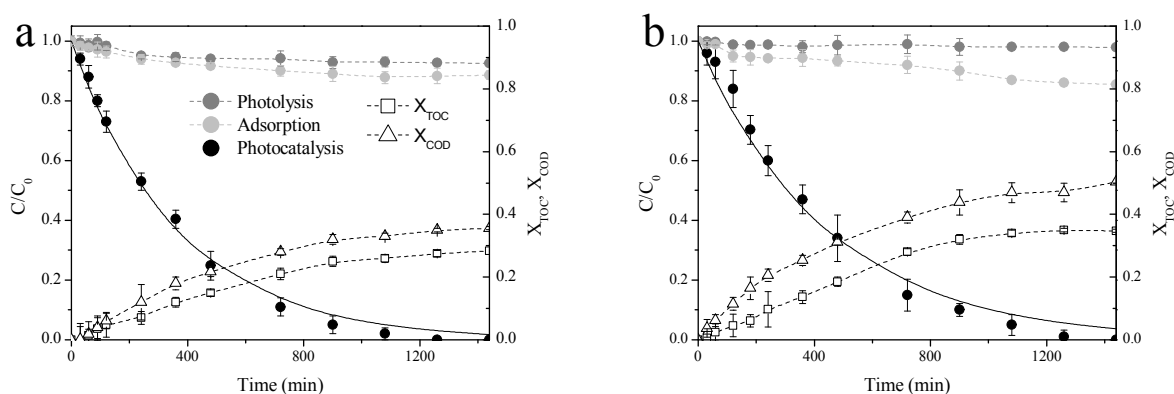


Figure 2. Time-course of ILs removal by adsorption, photolysis and photocatalysis, as well as COD removal and TOC conversion along photocatalytic degradation of BmpyrCl (a) and HmimCl (b). Symbols (experimental values) and solid lines (fitting values).

Adsorption of ILs on the photocatalyst surface reduced their concentration in the medium by less than 20%; also, non-catalytic photolysis was completely inefficient owing to the stability of the ILs (especially HmimCl) under solar irradiation. This result is consistent with previous findings of Bedia et al. (2019) regarding that imidazolium-based ILs are more stable than other IL families. Thus, pyridinium-based ILs form more ion-pair species than imidazolium-based ones,⁴⁶ which facilitates their cleavage by direct photolysis. Although the nature of the anion scarcely influences IL removal, halides are more stable under solar light than other hydrophobic anions.⁴⁷ Using the photocatalyst at variable concentrations from 0.1 to 1 g L⁻¹ revealed that the lower values resulted in incomplete IL removal, whereas the higher ones failed to increase mineralization of organic matter, probably as a result of the catalyst opacity preventing irradiation of the whole solution. A TiO₂ concentration of 0.25 g L⁻¹ allowed complete removal of the ILs within 24 h. The kinetics of ILs removal by several advanced oxidation processes has been usually described by a pseudo-first order equation, obtaining an appropriate fitting of the experimental results (Table 2). This kinetic model was used to describe the

oxidation process with rate constants values of $2.5 \cdot 10^{-3} \pm 1.3 \cdot 10^{-4} \text{ min}^{-1}$ ($R^2 = 0.996$) and $1.8 \cdot 10^{-3} \pm 1.7 \cdot 10^{-4} \text{ min}^{-1}$ ($R^2 = 0.991$) for BmpyrCl and HmimCl removal, respectively. These results indicated that the pyridinium core was easy to degrade by photocatalysis, which match with the high stability of imidazolium-based ILs under solar light irradiation. As expected, photocatalytic degradation rate was lower than those achieved for other oxidation processes as Fenton oxidation. In electro-oxidation processes, the values of the kinetics constants were similar to those obtained by photocatalytic oxidation, since the pollutant degradation occurred also slowly but with a great efficiency in terms of mineralization. Photocatalytic process seems not to be competitive according to the IL removal rate but allows reducing the cost of the treatment and becoming an environmental-friendly solution for the removal of refractory products to conventional biological processes. Several works found in the literature on pyridinium- and imidazolium-based ILs removal by photocatalytic oxidation under UV irradiation showed complete ILs degradation in most cases,^{25,27,28} observing a clear stability for smaller ILs.²⁶ The increase in alkyl-chain length of imidazolium-based ILs improved the cation degradation rate, despite the photocatalytic degradation of Bmpyr⁺ cation was also faster than imidazolium ones with greater molar weight.³¹

Table 2. Values of the kinetic constant for the degradation of imidazolium-based ILs for several advanced oxidation processes.

Process	Compound	k (min ⁻¹)	Reference
Photocatalysis	BmpyrCl	$2.5 \cdot 10^{-3}$	This work
	HmimCl	$1.8 \cdot 10^{-3}$	
Fenton	BmimCl	$5.6 \cdot 10^{-2}$	48
Fenton	BmpyrCl	$6.5 \cdot 10^{-2}$	18
	HmimCl	$2.9 \cdot 10^{-1}$	
Photocatalysis	BmimCl	$5.0 \cdot 10^{-3}$	30
CWPO	BmimCl	$2.5 \cdot 10^{-2}$	49

		Electrolysis: $6.1 \cdot 10^{-3}$	
Electrooxidation	BmimCl	Sonoelectrolysis: $8.2 \cdot 10^{-3}$	50
		Photoelectrolysis: $9.4 \cdot 10^{-3}$	

Photocatalytic degradation of BmpyrCl and HmimCl was also monitored through TOC conversion and COD removal. Although mineralization in terms of TOC conversion was similar with both compounds, Bmpyr⁺ was faster removed than the imidazolium-based IL. As can be seen in **Figure 2**, TOC and COD conversion were unrelated to IL removal efficiency. In fact, a complete degradation of BmpyrCl and HmimCl was reached after 24 h of irradiation whereas the degree of mineralization was less than 30%. This result clearly indicates that the parent compounds were transformed into byproducts that were refractory to photocatalytic oxidation (particularly aliphatic chains and nonaromatic compounds, which were not attacked by hydroxyl radicals).⁵¹ As expected, mineralization was less marked than COD removal because TOC was independent of the oxidation state of organic matter and no other substances such as hydrogen, nitrogen or inorganic compounds could be measured. However, such substances may also have been oxidized by photocatalysis and contributed to the change in COD.⁵²

Figure 3 shows the carbon and nitrogen mass balance closures for the photocatalytic degradation of BmpyrCl and HmimCl. An appreciable concentration of short-chain organic acids (viz., 35% and 42% TOC upon irradiation of Bmpyr⁺ and Hmim⁺, respectively) was obtained at long reaction times; the remaining TOC could be assigned to none of the byproducts identified, however. The carbon mass balance at short reaction times was better closed thanks to the presence of Hmim⁺ or Bmpyr⁺ cation. The concentration of unknown byproducts increased as the photocatalytic degradation reaction developed. The nitrogen mass balance closure was similar to the carbon mass

balance closure in terms of identified species. Although the reduction in total nitrogen was negligible (less than 5% of the initial TN value), nitrogen-containing species were transformed at the latest reaction stages as substantial concentrations of nitrite and nitrate were formed. It is worth noting the substantial contribution of ammonium nitrogen (N-NH_4^+) to the nitrogen balance by effect of the presence of double bonds (particularly $\text{C}=\text{N}$ bonds) in the parent compounds favoring the formation of NH_4^+ ions in the photocatalytic process.⁵³

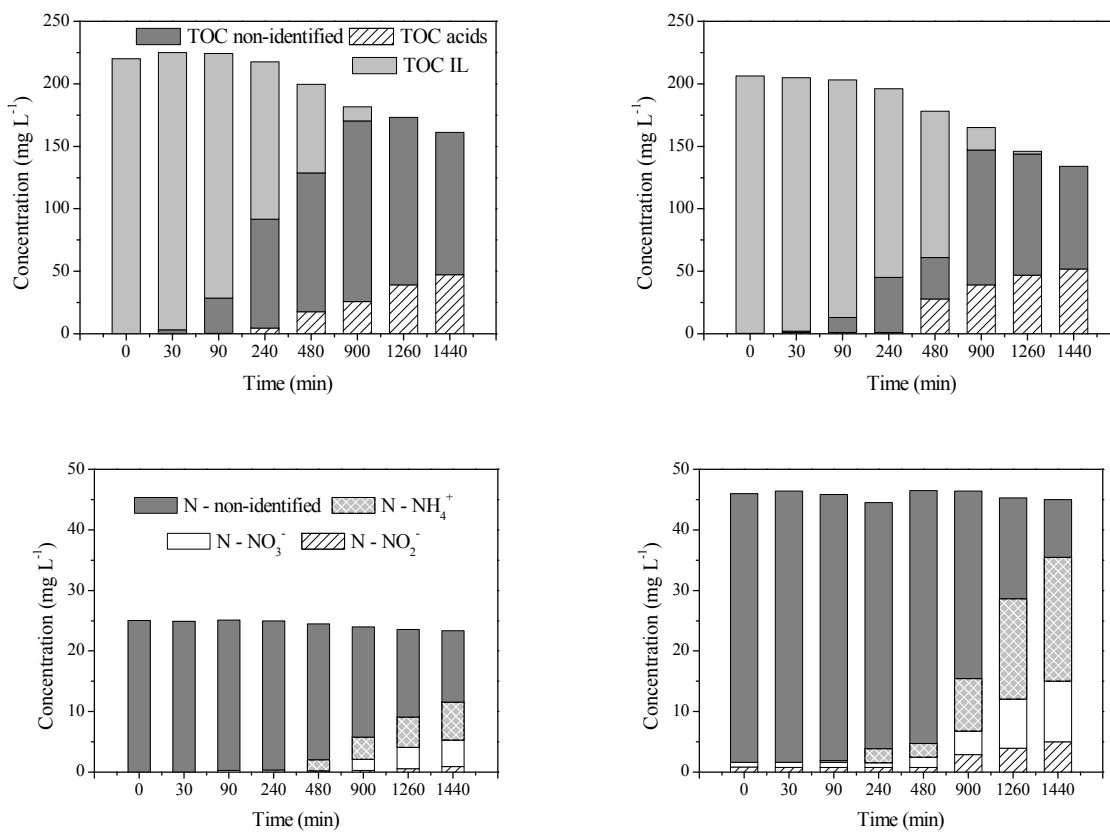
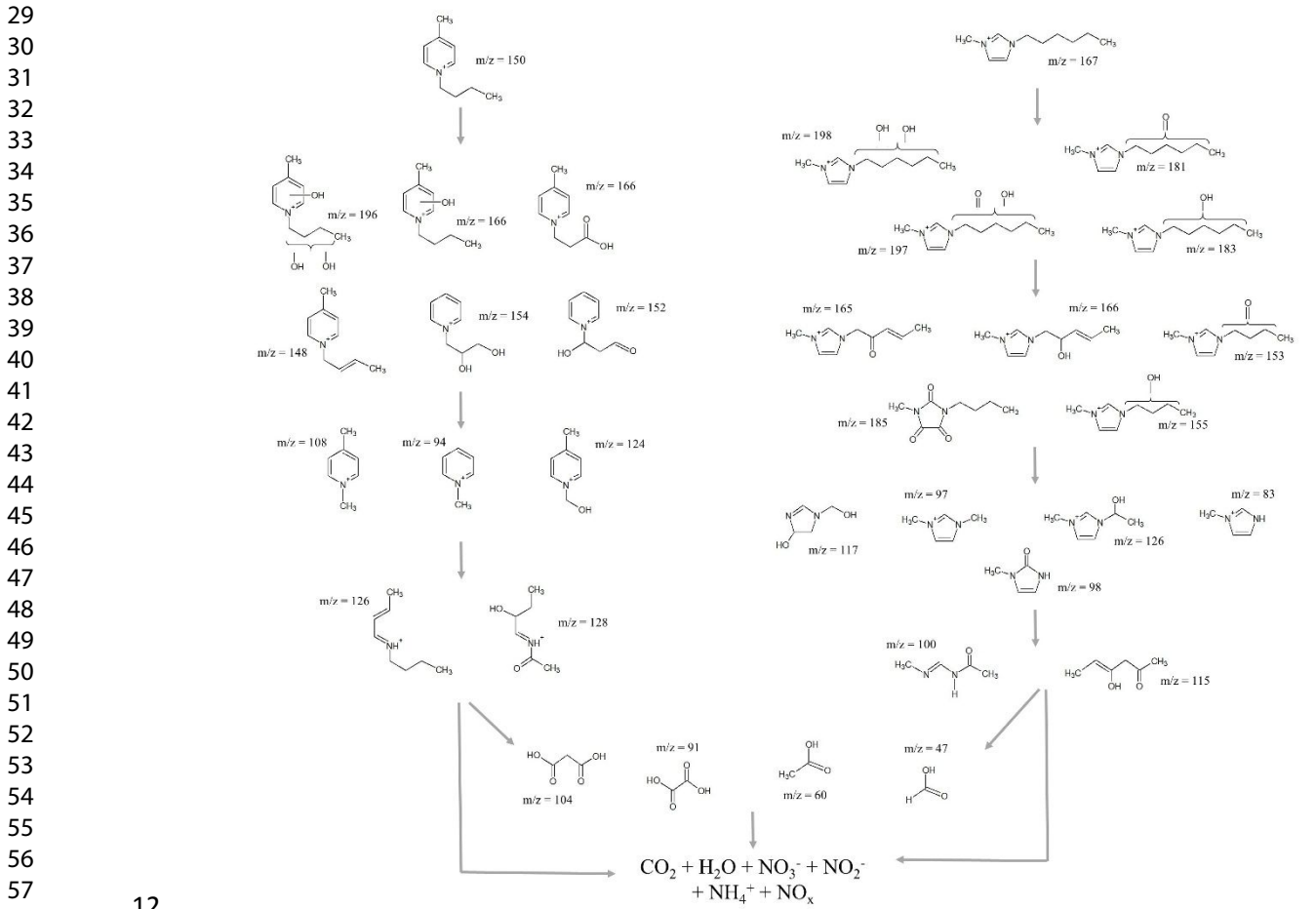


Figure 3. Evolution of the carbon and nitrogen balance closure of BmpyrCl (left) and HmimCl (right) upon photocatalytic oxidation.

The analysis of the effluents from the ILs photocatalytic oxidation by HPLC/MS allowed the identification of the degradation by-products depicted in Figure 4, according to m/z ratio. As expected, the initial samples were only composed by Bmpyr⁺ ($m/z = 150$) and

Hmim⁺ ($m/z = 167$), respectively. These parent compounds appeared in all the samples withdrawn along the experiment excluding the final ones. The variety of unidentified intermediates in the carbon balance closure increased with the irradiation time. According to the by-products detected, both ILs followed the same degradation steps. In the beginning, the hydroxyl radicals generated by photocatalytic oxidation caused the hydroxylation of the parent compounds, giving rise to molecules with higher molecular weight. Different species were likely formed through hydroxylation ($m/z = 183$), dihydroxylation ($m/z = 198$ and 196) or hydroxylation-reduction processes ($m/z = 181$, 197 and 166). Most of these intermediates reached a maximum concentration within 30-90 min, matching with the increase in ecotoxicity measured in those samples. The formation of transformation products with smaller mass was related with the imidazole or pyridine ring opening and the shortening of the alkyl-chain, involving the possible loss of a molecule of carbon dioxide and even ethylene molecule, a molecule that matched with the structure proposed with $m/z = 126$. The smaller transformation by-products exhibited less ecotoxicity than the parent compounds. The identified compounds in the final samples corresponded mostly to short-chain organic acids, which were oxidized to carbon dioxide, water and nitrogen species as NO_x .^{54,55} The major concentration of short-chain organic acids correlated with acetic and formic acids, in which the carbon-oxygen bond was considered as refractory to hydroxyl radicals attack, accumulating in the last stages of the oxidation process.⁵⁶ Although the photocatalytic degradation of ILs under solar light has been scarcely studied, some of the intermediates detected were previously described by other authors, indicating no dependence of the degradation pathway on the starting pyridinium or imidazolium-based IL to be removed. Thus, Calza et al. (2018) detected some intermediates depicted in **Figure 4** ($m/z = 154$, 152 and 94) from photocatalytic oxidation of several pyridinium-based ILs, and the by-product with $m/z =$

1 117 in case of imidazolium-based IL degradation.²⁸ The intermediates obtained
2 confirmed the non-selective attack of the hydroxyl radicals which, depending on the
3 breakage site, gave rise to different degradation compounds and avoided to predict the
4 exact route of generation of the low molecular weight transformation products.
5 Nevertheless, some of the intermediates were previously described as by-products of IL
6 degradation by using other advanced oxidation processes. The by-product with $m/z = 166$
7 was also identified during Fenton^{18,58} and electrocatalytic oxidation of BmpyrCl.⁵⁹
8 Gomez-Herrero et al. (2018) also found by-products with $m/z = 197$, 185, 98 and 97
9 during the degradation of HmimCl by Fenton reagent, while Siedlecka et al. (2013) and
10 Garcia-Segura et al. (2016) identified the by-products with $m/z = 185$ and 97 by anodic
11 oxidation of imidazolium-based ILs.

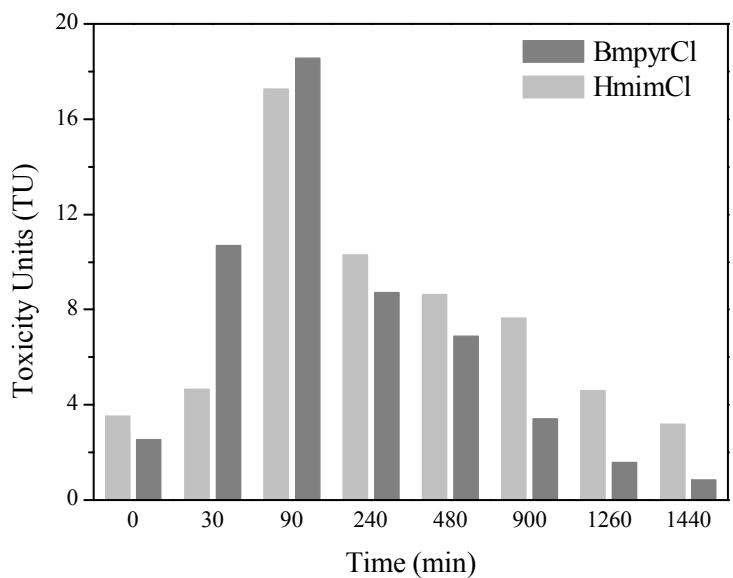


12
13 **Figure 4.** Reaction pathway for the photocatalytic degradation of BmpyrCl and HmimCl.

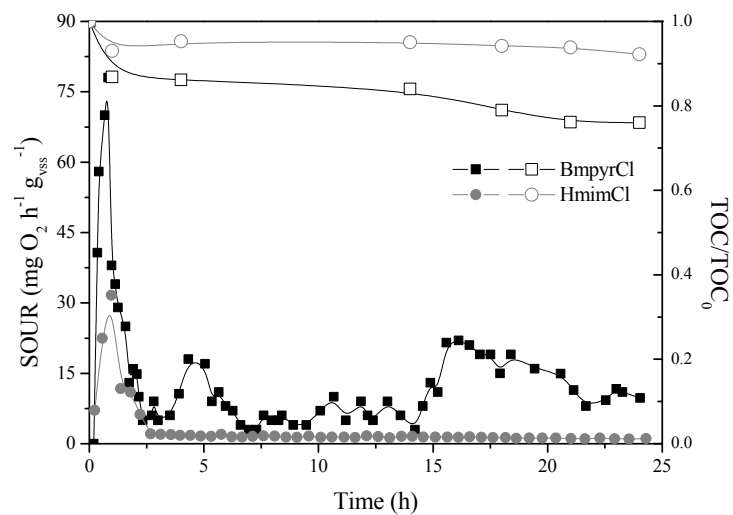
Figure 5 shows the time course of ecotoxicity during the photodegradation of BmpyrCl and HmimCl irradiated with solar light. The two ILs had moderate ecotoxicity level (3.53 for HmimCl and 2.22 for BmpyrCl, both of which are consistent with previously reported values).^{62,63} As elongation of the alkyl-chain increases toxicity in imidazolium-based ILs, HmimCl was more ecotoxic than BmpyrCl, despite pyridinium-based ILs constitute one of the most ecotoxic families. As can be seen in **Figure 5**, the ecotoxicity of the effluents from the photocatalytic degradation of BmpyrCl and HmimCl increased at the early reaction stages. Thus, the intermediates identified at a reaction time of 90 min, where ecotoxicity peaked, showed m/z values of 166, 154, 152 and 148 for BmpyrCl, and m/z values of 198, 197, 185 and 183 for HmimCl. These results are consistent with the presence of complex structures of potentially high ecotoxicity. As the photocatalytic reaction developed, ecotoxicity rapidly decreased through breakdown of imidazolium and pyridinium rings (linear forms are usually less toxic than are aromatic compounds).⁶⁴ A similar trend was observed by Calza et al. (2015), who found a maximum of ecotoxicity after 2 h of irradiation. As expected, the resulting effluents upon photocatalytic oxidation were not ecotoxic⁵⁸ and can be biologically treated without damaging the microorganisms or destabilizing the bioreactor.⁶⁵

Biological oxygen demand (BOD₅) was measured in both the initial aqueous solutions and the effluents from the photocatalytic oxidation of the ILs. Based on their biodegradability index, BmpyrCl and HmimCl were both classified as non-biodegradable; in fact, their BOD₅/COD ratios were lower than 0.05. However, these ratios increased with time to values around 0.3–0.4, so the effluents were deemed biodegradable.⁶⁶ The

1 increased biodegradability obtained, and the low ecotoxicity of the IL oxidation products,
2 allowed the effluents to be biologically treated.



4
5 **Figure 5.** Time course of ecotoxicity in the photodegradation of BmpyrCl and HmimCl under
6 solar light irradiation.



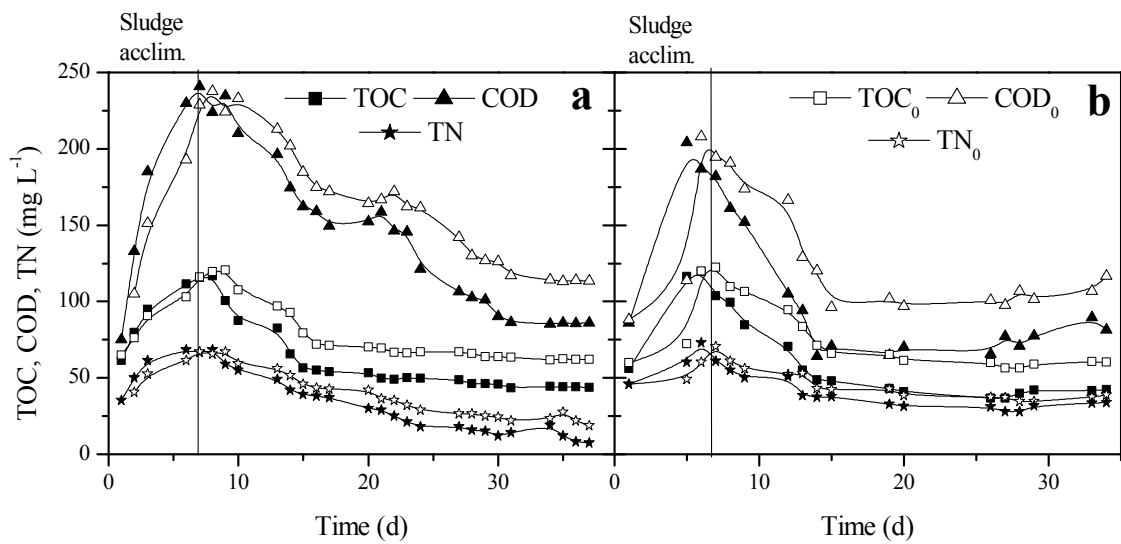
8
9 **Figure 6.** SOUR (filled symbols) and TOC evolution (empty symbols) of Bmpyr and Hmim
10 effluents from photocatalytic degradation of Bmpyr and Hmim, during the fast biodegradability
11 test.

1 The biodegradability of the effluents from the photocatalytic degradation of BmimCl and
2 HmimCl was assessed from respirometric measurements. **Figure 6** shows the
3 respirometric profile of the effluents in term of changes in specific oxygen uptake rate
4 (SOUR) and TOC. As can be seen, SOUR initially increased by effect of the presence of
5 biodegradable compounds such as short-chain organic acids as a result of microbial
6 metabolism involving oxygen consumption. Removing easily biodegraded compounds
7 also reduced TOC, albeit only slightly. The variation of SOUR and TOC in the HmimCl
8 effluent exhibited a plateau after 3 h of reaction suggesting the absence of other
9 biodegradable compounds in the medium. On the other hand, the SOUR profile for the
10 Bmpyr⁺ effluent exhibited an additional peak after 15 h, probably due to the presence of
11 partially biodegradable intermediates that required acclimation of microorganisms in the
12 activated sludge before they could be consumed.

13 The effluents from the photocatalytic oxidation of BmpyrCl and HmimCl were subjected
14 to biological treatment in a sequential batch reactor. The bioreactor operated in 8 h cycles
15 and was supplied with no additional carbon or nitrogen sources in order to ensure that
16 only organic matter present in the effluents would be degraded. **Figure 7** shows TOC,
17 COD and TN as measured at the beginning and end of consecutive cycles, until a steady
18 state in terms of organic matter removal was reached. As can be seen, products
19 accumulated over the first few days owing to the need for the sludge to accommodate
20 before partially biodegradable compounds present in the effluent started to be removed.
21 Once the sludge began to degrade organic matter, TOC, COD and TN decreased
22 throughout the biological treatment. Changes in TOC, and hence in mineralization, were
23 similar in both effluents. However, COD in the effluent from HmimCl photocatalysis
24 exhibited a pronounced decrease leading to a plateau after 15 days of treatment, whereas
25 the BmpyrCl effluent took 30 d to reach the steady state. Therefore, degradation of the

1
2
3
4
5
6
7
8
9
10
11
12
13
14
15
16
17
18
19
20
21
22
23
24
25
26
27
28
29
30
31
32
33
34
35
36
37
38
39
40
41
42
43
44
45
46
47
48
49
50
51
52
53
54
55
56
57
58
59
60

1 by-products present in the effluent from HmimCl oxidation was seemingly faster by effect
2 of its increased content in short-chain organic acids and readily biodegraded
3 intermediates (**Figure 3**). The decrease in TN matched the COD reduction profile for both
4 IL effluents. The decreased organic matter content found on equal TOC values in the
5 Bmpyr⁺ effluent is suggestive of the presence of intermediates releasing nitrogen species.
6 The residual values of TOC, COD and TN at the end of the biological treatment can be
7 ascribed to the presence of byproducts refractory to biodegradation or even to their
8 potentially toxic effects on the sludge inducing cell lysis and the release of intracellular
9 content to the SBR, thereby increasing the amount of carbon available.⁶⁷



10

11 **Figure 7.** Evolution of initial (empty) and final (filled) COD, TOC and TN during biological
12 treatment of effluents from photocatalytic oxidation of BmpyrCl (a) and HmimCl (b)

13

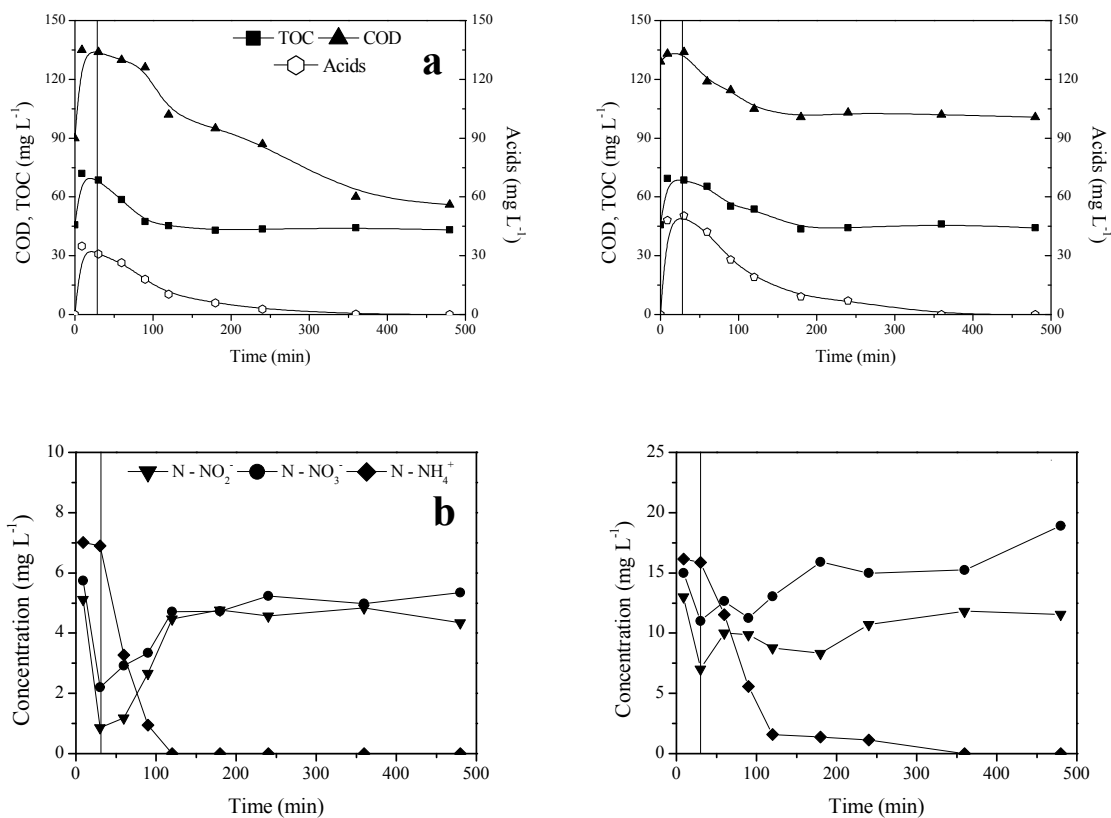
14 Once the steady state was reached, biodegradation over an SBR cycle was examined
15 through the evolution of short-chain organic acids and nitrogen species, COD and TOC.
16 As can be seen in **Figure 8**, TOC decreased markedly in the first few hours of the cycle
17 by effect of degradation of short-chain organic acids (acetic and formic, mainly) present
18 in the influent. Once completion of the aerobic reaction was confirmed by the constancy

in TOC, biodegradation of the intermediates was negligible as the likely result of their containing aromatic rings impossible to degrade by the activated sludge. However, the low ecotoxicity of the effluent allowed the adapted sludge to retain its ability to degrade readily biodegraded compounds such as acetic and formic acids. As noted earlier, although TOC remained constant after short-chain organic acids were removed from the Bmpyr⁺ effluent, COD continued to decrease through the end of the cycle, probably because some intermediates were converted into inorganic species without reducing the carbon content.

As regards nitrogen species, nitrate and nitrite contents decreased over the anoxic period, probably through heterotrophic denitrification for nitrate reduction and the release of N₂ to the atmosphere. On the other hand, the concentration of ammonia remained constant over the anoxic stage and decreased at the aerobic stage,⁶⁸ which is consistent with an increase in nitrate and nitrite levels due to the transformation of ammonia into both ions. In addition, the high concentration of unknown nitrogen-containing species suggests that the intermediates were not biodegradable, probably because they contained aromatic rings refractory to the biological treatment. However, using alternate aerobic–anoxic stages in the bioreactor facilitated the removal of inorganic species such as nitrogen.^{69,70} Also, in absence of oxygen, the presence of carbon and nitrogen sources in the effluents favored denitrification and boosted substrate consumption in the subsequent aerobic stage in each SBR cycle.⁷¹

Coupling photocatalytic oxidation and a biological treatment in a SBR led to TOC conversion above 78% and 75% for BmpyrCl and HmimCl, respectively, despite only a 28% and 34 % of TOC conversion was obtained after photocatalytic oxidation, due to the formation of refractory by-products to the attack of hydroxyl radical. As pyridinium– and

imidazolium-based ILs are considered no biodegradable compounds,¹⁸ a synergistic effect was observed, since the effluents of the combined treatment presented a degree of mineralization higher than those obtained by each process individually.



5

Figure 8. Time course of TOC, COD and short-chain organic acids (a) and nitrogen inorganic species (b) over a 8-h SBR cycle for the effluents from photocatalysis oxidation of BmpyrCl (left) and HmimCl (right).

9

4. Conclusions

Coupling a sequential photocatalytic oxidation and a biological treatment improved the removal of HmimCl and BmpyrCl. Photolysis and adsorption of both ILs were almost negligible. By contrast, photocatalytic oxidation produced effluents free of Hmim⁺ and Bmpyr⁺ and containing substantial amounts of biodegradable compounds such as short-chain organic acids, which are less ecotoxic and easier to remove by microbial

metabolism than the parent compounds. Biodegradability and ecotoxicity tests allowed the best photocatalytic conditions for the combined treatment to be established.

Aerobic oxidation of the effluents from the photocatalytic degradation of the ILs in a bioreactor (SBR) boosted COD and TOC removal after an acclimation period (5–10 d) of the activated sludge. The two oxidation processes in combination led to overall COD and TOC conversions of 75% for Hmim⁺ and 78% for Bmpyr⁺, which are considerably higher than the values obtained with either individual treatment. In addition, microbial activity in the SBR cycles enabled complete biodegradation of short-chain organic acids in addition to the release of inorganic species with slightly decreased concentrations of unknown intermediates.

Acknowledgements

The authors wish to thank the Spanish MINECO and Comunidad de Madrid for the financial support through the projects CTM2016-76564-R and BIOTRES-CM (S2018/EMT-4344), respectively.

References

1. Welton T. Room-Temperature Ionic Liquids. Solvents for Synthesis and Catalysis. *Chem. Rev* **99**: 2071–2084 (1999).
2. Couling DJ, Bernot RJ, Docherty KM, Dixon K and Maginn EJ. Assessing the factors responsible for ionic liquid toxicity to aquatic organisms via quantitative structure – property relationship modeling. *Green Chem.* **8**: 82–90 (2006).
3. Fredlake CP, Crosthwaite JM, Hert DG, Aki SNVK and Brennecke JF. Thermophysical Properties of Imidazolium-Based Ionic Liquids. *J. Chem. Eng.*

- 1
2
3 1 *Data* **49**: 954–964 (2004).
4
5
6 2 4. Rogers RD and Seddon KR. Ionic Liquids - Solvents of the Future? *Science*. **302**:
7
8 3 792–793 (2003).
9
10
11 4 5. Ohno H. Functional design of ionic liquids. *Bull. Chem. Soc. Jpn.* **79**: 1665–1680
12
13 5 (2006).
14
15
16 6 6. Hallett JP and Welton T. Room-Temperature Ionic Liquids : Solvents for Synthesis
17
18 and Catalysis. *Chem. Rev* **2**: 3508–3576 (2011).
19
20
21
22 8 7. Palomar J, Gonzalez-miquel M, Bedia J, Rodriguez F and Rodriguez JJ. Task-
23
24 9 specific ionic liquids for efficient ammonia absorption. *Sep. Purif. Technol.* **82**:
25
26 10 43–52 (2011).
27
28
29 11 8. Plechkova NV and Seddon KR. Applications of ionic liquids in the chemical
30
31 12 industry. *Chem Soc Rev* **37**: 123–150 (2008).
32
33
34 13 9. Markiewicz M, Piszora M, Caicedo N, Jungnickel C and Stolte S. Toxicity of ionic
35
36 14 liquid cations and anions towards activated sewage sludge organisms from
37
38 15 different sources e Consequences for biodegradation testing and wastewater
39
40 16 treatment plant operation. *Water Res.* **47**: 2921–2928 (2013).
41
42
43
44 17 10. Neumann J, Steudte S, Cho C-W, Thöming J and Stolte S. Biodegradability of 27
45
46 18 pyrrolidinium, morpholinium, piperidinium, imidazolium and pyridinium ionic
47
48 19 liquid cations under aerobic conditions. *Green Chem.* **16**: 2174–2184(2014).
49
50
51
52 20 11. Romero A, Santos A, Tojo J and Rodríguez A. Toxicity and biodegradability of
53
54 21 imidazolium ionic liquids. *J. Hazard. Mater.* **151**: 268–273 (2008).
55
56
57 22 12. Cho C, Jeon Y-C, Pham TPT, Vijayaraghavan K and Yun Y-S. The ecotoxicity of
58
59 23 ionic liquids and traditional organic solvents on microalga *Selenastrum*

- 1 *capricornutum*. *Ecotox Environ Saf.* **71**: 166–171 (2008).
- 2
- 3 13. Biczak R, Pawłowska B, Bałczewski P and Rychter P. The role of the anion in the
- 4
- 5 toxicity of imidazolium ionic liquids. *J. Hazard. Mater.* **274**: 181–190 (2014).
- 6
- 7
- 8 14. Tsarpali V and Dailianis S. [omim][BF₄]⁻-mediated toxicity in mussel
- 9
- 10 hemocytes includes its interaction with cellular membrane proteins. *Aquatic*
- 11
- 12 *Toxicol* **203**: 88–94 (2018).
- 13
- 14
- 15 15. Docherty KM and Kulpa CF. Toxicity and antimicrobial activity of imidazolium
- 16
- 17 and pyridinium ionic liquids. *Green Chem.* **4**: 185–189 (2005).
- 18
- 19
- 20 16. Ventura SPM, Gonc AMM, Gonc F and Coutinho JAP. Assessing the toxicity on
- 21
- 22 [C₃mim][Tf₂N]⁻ to aquatic organisms of different trophic levels. *Aquatic*
- 23
- 24 *Toxicol.* **96**: 290–297 (2010).
- 25
- 26
- 27 17. Siedlecka EM, Stolte S, Golebiowski M, nienstedt A, Stepnowski P and Thoming
- 28
- 29 J. Advanced oxidation process for the removal of ionic liquids from water: The
- 30
- 31 influence of functionalized side chains on the electrochemical degradability of
- 32
- 33 imidazolium cations. *Sep. Purif. Technol.* **101**: 26–33 (2012).
- 34
- 35
- 36 18. Gomez-Herrero E, Tobajas M, Polo A, Rodriguez JJ and Mohedano AF. Removal
- 37
- 38 of imidazolium- and pyridinium-based ionic liquids by Fenton oxidation. *Environ*
- 39
- 40 *Sci Pol Res.* **35**: 34930–34937 (2018).
- 41
- 42
- 43 19. Oxley JD, Prozorov T and Suslick KS. Sonochemistry and Sonoluminescence of
- 44
- 45 Room-Temperature Ionic Liquids. *J Am Chem Soc.* **125**: 11138–11139 (2003).
- 46
- 47
- 48 20. Jiang L, Yuan X, Zeng G, Wu Z and Liang J. Applied Catalysis B : Environmental
- 49
- 50 Metal-free e ffi cient photocatalyst for stable visible-light photocatalytic
- 51
- 52 degradation of refractory pollutant. *Appl. Catal. B Environ.* **221**: 715–725 (2018).
- 53
- 54
- 55
- 56
- 57
- 58
- 59
- 60

- 1
2
3 1 21. Ohtani B. Journal of Photochemistry and Photobiology C: Photochemistry
4
5 2 Reviews Photocatalysis A to Z — What we know and what we do not know in a
6
7 3 scientific sense. *Journal Photochem. Photobiol. C Photochem. Rev.* **11**: 157–178
8
9 4 (2011).
10
11
12
13 5 22. Sanchez M, Rivero MJ and Ortiz I. Photocatalytic oxidation of grey water over
14
15 6 titanium dioxide suspensions. *Desalination* **262**: 141–146 (2010).
16
17
18 7 23. Ribao P, Rivero MJ and Ortiz I. Enhanced photocatalytic activity using GO/TiO₂
19
20 8 catalyst for the removal of DCA solutions. *Environ. Sci. Pollut. Res.* **25**: 34893–
21
22 9 34902 (2018).
23
24
25
26 10 24. Sanchez M, Rivero MJ and Ortiz I. Kinetics of dodecylbenzenesulphonate
27
28 11 mineralisation by TiO₂ photocatalysis. *Appl. Catal. B Environ.* **101**: 515–521
29
30 12 (2011).
31
32
33 13 25. Stepnowski P and Zaleska A. Comparison of different advanced oxidation
34
35 14 processes for the degradation of room temperature ionic liquids. *J Photochem*
36
37 15 *Photobiol A: Chem.* **170**: 45–50 (2005).
38
39
40
41 16 26. Morawski A, Janus M, Goc-Maciejewska I, Syguda A and Pernak J.
42
43 17 Decomposition of Ionic Liquids by Photocatalysis. *Pol. J. Chem.* **79**: 1929–1935
44
45 18 (2005).
46
47
48 19 27. Itakura T, Hirata AK and Aoki AM. Decomposition and removal of ionic liquid in
49
50 20 aqueous solution by hydrothermal and photocatalytic treatment. *Environ Chem*
51
52 21 *Letters.* **7**: 343–345 (2009).
53
54
55
56 22 28. Calza P, Vione D, Fabbri D, Aigotti R and Medana C. Imidazolium-Based Ionic
57
58 23 Liquids in Water: Assessment of Photocatalytic and Photochemical
59
60

- Transformation. *Environ Sci Technol.* **49**: 10951–10958 (2015).
29. Calza P, Fabbri D, Noè G, Santoro V and Medana C. Assessment of the photocatalytic transformation of pyridinium-based ionic liquids in water. *J. Hazard. Mater.* **341**: 55–65 (2018).
30. Leonardo da Silva W. *et al.* Separation and Purification Technology Petrochemical residue-derived silica-supported titania-magnesium catalysts for the photocatalytic degradation of imidazolium ionic liquids in water. *Sep. Purif. Technol.* **218**: 191–199 (2019).
31. Bedia J, Rodriguez JJ, Moreno D, Palomar J and Belver C. Photostability and photocatalytic degradation of ionic liquids in water under solar light. *RSC Adv.* **9**: 2026–2033 (2019).
32. Ventura PM, Marques CS, Rosatella AA, Afonso CAM and Gonc F. Ecotoxicology and Environmental Safety Toxicity assessment of various ionic liquid families towards *Vibrio fischeri* marine bacteria. *Ecotox Environ Saf.* **76**: 162–168 (2012).
33. Liwarska-Bizukojc E, Maton C and Stevens CV. Biodegradation of imidazolium ionic liquids by activated sludge microorganisms. *Biodegradation* **26**: 453–463 (2015).
34. Docherty KM, Dixon JK and Kulpa CF. Biodegradability of imidazolium and pyridinium ionic liquids by an activated sludge microbial community. *Biodegradation* **18**: 481–493 (2007).
35. Wu Y, Li T and Yang L. Bioresource Technology Mechanisms of removing pollutants from aqueous solutions by microorganisms and their aggregates: A

- 1 review. *Bioresour. Technol.* **107**: 10–18 (2012).
- 2
- 3 1
- 4
- 5
- 6 2 36. Pérez-Farías C, Fernández Mohedano A, Díaz Nieto E and Moreno-Andrade I.
- 7
- 8 Bioaumentación De Un Bioreactor Discontinuo Para La Degradación De Agua
- 9
- 10
- 11 4 Residual Conteniendo Un Líquido Iónico. *Rev. AIDIS Ing. y Ciencias Ambient.*
- 12
- 13 5 *Investig. Desarro. y práctica* **10**: 61–72 (2017).
- 14
- 15
- 16 6 37. Khare UK, Bose P and Vankar PS. Impact of ozonation on subsequent treatment
- 17
- 18 7 of azo dye solutions. *J Chem Technol Biotechnol* **1022**: 1012–1022 (2007).
- 19
- 20
- 21 8 38. Pulgarin C. *et al.* Strategy for the coupling of photochemical and biological flow
- 22
- 23 9 reactors useful in mineralization of biorecalcitrant industrial pollutants. *Catal*
- 24
- 25 *Today* **54**: 341–352 (1999).
- 26
- 27 10
- 28
- 29 11 39. Oller I, Malato S and Sánchez-pérez JA. Science of the Total Environment
- 30
- 31 12 Combination of Advanced Oxidation Processes and biological treatments for
- 32
- 33 13 wastewater decontamination — A review. *Sci. Total Environ.* **409**: 4141–4166
- 34
- 35 14 (2011).
- 36
- 37
- 38
- 39 15 40. Ballesteros Martín MM, Sánchez Pérez JA, Casas López JL, Oller I and Malato
- 40
- 41 16 Rodríguez S. Degradation of a four-pesticide mixture by combined photo-Fenton
- 42
- 43 17 and biological oxidation. *Water Res.* **43**: 653–660 (2009).
- 44
- 45
- 46 18 41. Sanchis S, Polo AM, Tobajas M, Rodriguez JJ and Mohedano AF. Degradation of
- 47
- 48 19 chlorophenoxy herbicides by coupled Fenton and biological oxidation.
- 49
- 50 20 *Chemosphere* **93**: 115–122 (2013).
- 51
- 52
- 53
- 54 21 42. Sirtori C, Zapata A, Oller I, Gernjak W and Agu A. Decontamination industrial
- 55
- 56 22 pharmaceutical wastewater by combining solar photo-Fenton and biological
- 57
- 58 23 treatment. *Water Res* **43**: 661–668 (2009).
- 59
- 60

- 1
2
3 1 43. Gomez-Herrero E, Tobajas M, Polo A, Rodriguez JJ and Mohedano AF. Removal
4
5 of imidazolium-based ionic liquid by coupling Fenton and biological oxidation. *J.*
6
7 *Hazard. Mater.* **365**, 289–296 (2019).
8
9
10 4 44. Jiang L, Yuan X, Zeng G, Wu Z and Liang J. Applied Catalysis B : Environmental
11
12 Metal-free efficient photocatalyst for stable visible-light photocatalytic
13
14 degradation of refractory pollutant. *Appl. Catal. B Environ.* **221**, 715–725 (2018).
15
16
17 7 45. Polo AM, Tobajas M, Sanchis S, Mohedano AF and Rodríguez JJ. Comparison of
18
19 experimental methods for determination of toxicity and biodegradability of
20
21 xenobiotic compounds. *Biodegradation* **22**, 751–761 (2011).
22
23
24 10 46. Binetti E. *et al.* Spectroscopic Study on Imidazolium-Based Ionic Liquids: Effect
25
26 of Alkyl Chain Length and Anion. *J Phys Chem B* **116**: 3512–3518 (2012).
27
28
29 12 47. Li W. *et al.* Effect of Water and Organic Solvents on the Ionic Dissociation of
30
31 Ionic Liquids. *J Phys Chem B* **111**:6452–6456 (2007).
32
33
34 14 48. Siedlecka EM, Mroziak W, Kaczyński Z and Stepnowski P. Degradation of 1-butyl-
35
36 3-methylimidazolium chloride ionic liquid in a Fenton-like system. *J. Hazard.*
37
38 *Mater.* **154**, 893–900 (2008).
39
40
41 17 49. Mena IF. *et al.* Catalytic wet peroxide oxidation of imidazolium-based ionic
42
43 liquids : Catalyst stability and biodegradability enhancement. *Chem. Eng. J.* 1–10
44
45 (2018).
46
47
48 20 50. Mena IF. *et al.* Sono- and photoelectrocatalytic processes for the removal of ionic
49
50 liquids based on the 1-butyl-3-methylimidazolium cation. *J. Hazard. Mater.* **372**,
51
52 77–84 (2019).
53
54
55 23 51. Buxton GV, Greenstock CL, Hellman WP and Ross AB. Critical Review of rate
56
57
58
59
60

- 1 constants for reactions of hydrated electrons, hydrogen atoms and hydroxyl
2 radicals ($\cdot\text{OH}/\cdot\text{O}^-$ in Aqueous Solution. *J. Phys. Chem. Ref. Data* **17**: 513–886
3 (1988).
- 4 52. Kaabeche ONEH, Zouaghi R, Boukhedoua S, Bendjabeour S and Sehili T. A
5 Comparative study on Photocatalytic Degradation of Pyridinium-Based Ionic
6 Liquid by TiO_2 and ZnO in Aqueous Solution. *Int. J. Chem. React. Eng.* **17**: 1–14
7 (2019).
- 8 53. Calza P, Pelizzetti E and Minero C. The fate of organic nitrogen in photocatalysis :
9 an overview. *J Appl Electrochem* **35**: 665–673 (2005).
- 10 54. Vidales MJM De, Millán M, Sáez C, Cañizares P and Rodrigo MA.
11 Electrochemistry Communications What happens to inorganic nitrogen species
12 during conductive diamond electrochemical oxidation of real wastewater?
13 *Electrochem. commun.* **67**, 65–68 (2016).
- 14 55. Garcia-segura S, Mostafa E and Baltruschat H. Applied Catalysis B :
15 Environmental Could NO_x be released during mineralization of pollutants
16 containing nitrogen by hydroxyl radical ? Ascertaining the release of N-volatile
17 species. *"Applied Catal. B, Environ.* **207**, 376–384 (2017).
- 18 56. Zazo JA, Casas JA, Mohedano AF, Gilarranz MA and Rodríguez JJ. Chemical
19 pathway and kinetics of phenol oxidation by Fenton's reagent. *Environ. Sci.*
20 *Technol.* **39**: 9295–9302 (2005).
- 21 57. Calza P, Fabbri D, Noè G, Santoro V and Medana C. Assessment of the
22 photocatalytic transformation of pyridinium-based ionic liquids in water. *J.*
23 *Hazard. Mater.* **341**, 55–65 (2018).

- 1
2
3 1 58. Munoz M. *et al.* Ionic liquids breakdown by Fenton oxidation. *Catal Today* **240**:
4 16–21 (2015).
5
6 2
7
8 3 59. Pieczyska A. *et al.* A comparative study of electrochemical degradation of
9 imidazolium and pyridinium ionic liquids: A reaction pathway and ecotoxicity
10 evaluation. *Sep. Purif. Technol.* **156**: 522–534 (2015).
11
12 4
13 5
14
15 6 60. Siedlecka EM. *et al.* Electrocatalytic oxidation of 1-butyl-3-methylimidazolium
16 chloride: Effect of the electrode material. *Int. J. Electrochem. Sci.* **8**, 5560–5574
17
18 7
19
20 8
21
22
23 9 61. Garcia-Segura S, Lima ÁS, Cavalcanti EB and Brillas E. Anodic oxidation,
24 electro-Fenton and photoelectro-Fenton degradations of pyridinium- and
25 imidazolium-based ionic liquids in waters using a BDD/air-diffusion cell.
26 10
27
28 11
29
30 12
31
32
33 13 62. Montalbán MG, Hidalgo JM, Collado-González M, Díaz Baños FG and Villora,
34 G. Assessing chemical toxicity of ionic liquids on *Vibrio fischeri*: Correlation with
35
36 14
37
38 15
39
40
41 16 63. Costa SPF. *et al.* The aquatic impact of ionic liquids on freshwater organisms.
42
43 17
44
45
46 18 64. Ranke J, Stolte S, Sto R, Arning J and Jastorff B. Design of Sustainable Chemical
47 Products s The Example of Ionic Liquids. *Chem Rev* **107**: 2183–2206 (2007).
48
49 19
50
51 20 65. Tamer E. *et al.* Sequential UV – biological degradation of chlorophenols.
52
53 21
54
55
56 22 66. Momani FAI, Sans C, Contreras S and Esplugas S. Degradation of 2 , 4-
57
58
59 23
60

- 1
2
3 1 Treatment. *Water Environ Res* **78**: 590–597 (2002).
4
5
6 2 67. Monsalvo VM, Tobajas M, Mohedano AF and Rodriguez JJ. Intensification of
7
8 3 sequencing batch reactors by cometabolism and bioaugmentation with
9
10 4 *Pseudomonas putida* for the biodegradation of 4-chlorophenol. *J. Chem. Technol.*
11
12 *Biotechnol.* **87**: 1270–1275 (2012).
13
14
15
16 6 68. Diya BH. *et al.* Hybrid of Fenton and sequencing batch reactor for petroleum
17
18 7 refinery wastewater treatment. *J Industrial Engin Chem* **25**: 186–191 (2015).
19
20
21 8 69. Tobajas M, Polo AM, Monsalvo VM, Mohedano AF and Rodriguez JJ. Analysis
22
23 9 of the operating conditions in the treatment of cosmetic wastewater by sequencing
24
25 10 batch reactors. *Environ Engin Manag J* **13**: 2955–2962 (2014).
26
27
28
29 11 70. Zanetti L. *et al.* Progress in real-time control applied to biological nitrogen removal
30
31 12 from wastewater. A short-review. *Desalination* **286**: 1–7 (2012).
32
33
34 13 71. Jena J, Kumar R, Dixit A and Das T. Anoxic – aerobic SBR system for nitrate ,
35
36 14 phosphate and COD removal from high-strength wastewater and diversity study of
37
38 15 microbial communities. *Biochem Engin J* **105**, 80–89 (2016).
39
40
41
42 16
43
44
45 17
46
47
48
49
50
51
52
53
54
55
56
57
58
59
60